

Sol-gel template synthesis and photocatalytic behaviour of anatase titania nanoparticles

Vorrada Loryuenyong^{a,b,*}, Kunmutta Angamnuaysiri^a, Jidlada Sukcharoenpong^a, Athijit Suwannasri^a

^a Department of Materials Science and Engineering, Faculty of Engineering and Industrial Technology, Silpakorn University, Nakhon Pathom 73000 Thailand

^b National Centre of Excellence for Petroleum, Petrochemicals and Advanced Materials, Chulalongkorn University, Bangkok 10330 Thailand

*Corresponding author, e-mail: vorrada@gmail.com, vorrada@su.ac.th

Received 4 Feb 2012

Accepted 1 May 2012

ABSTRACT: In this study, titania nanoparticles were successfully prepared by a sol-gel template method, employing cetyltrimethylammonium bromide (CTAB) and CaCO₃ nanoparticles as templates. Titanium(IV) tetraisopropoxide and ethanol were used as a titanium precursor and alcoholic solvent, respectively. The obtained nanosized-titania was characterized by X-ray diffraction, transmission-electron microscopy, and N₂ adsorption and desorption methods. The photocatalytic activity of titania was investigated from the photodegradation of methylene blue solution under UVC irradiation. The results indicated that the amount of anatase crystallites and pore characteristics were important factors influencing the degree of photocatalysis of titania nanoparticles. Highly crystalline anatase titania could be obtained through the controlled hydrolysis reaction rate and the formation of loose-packed titania nanoparticles, while high specific surface area could be achieved with a template method.

KEYWORDS: sol-gel processes, TiO₂, cetyltrimethylammonium bromide, CaCO₃, BET

INTRODUCTION

Recently, nanocrystalline titania (TiO₂) has attracted tremendous attentions as a promising material for a wide range of applications such as photocatalysts, dye sensitized solar cells, and sensor devices^{1–3}. This is due to its unique and novel properties including high photocatalytic activity, high refractive index, low cost, non-toxicity, and large energy bandgap. One of the most useful aspects of titania is its use as a photocatalyst for the degradation of organic pollutants. The photocatalytic activity of titania depends on its morphology, particle size and distribution, porosity, crystallinity, and crystal structures. Among three crystalline polymorphs of titania (anatase, rutile, and brookite), anatase, and unstable brookite phases usually exhibit high photocatalytic activities, while rutile has the highest chemical stability^{4–8}. As a result, well-structured anatase titania with high specific surface area favours photocatalytic activity.

The most common technique used to synthesize mesoporous and nanocrystalline titania is the sol-gel method, in which titania nanoparticles are prepared by hydrolysis and polycondensation reactions of titanium precursors such as titanium alkoxides. The properties of the synthesized nanoparticles can

be tailored through processing parameters such as pH, reaction temperature, catalysts, concentration and precursor molar ratio. The main factors influencing the degradation of organic materials with titania photocatalysts follow the following orders of significance: type of stabilizer > type of solvent > calcination temperature⁹. In addition, many studies^{10,11} have also been focused onto the controllable hydrolysis rate of titanium alkoxide. This is because high hydrolysis rate may cause uncontrolled precipitation and the formation of rutile phase, resulting in poor photocatalytic activity¹². In general, the alkoxide hydrolyses quickly in water, and thus alcohol is often used as a solubilizing agent to slow down the reaction and to provide a homogeneous environment for particle growth¹³.

In the past decades, a number of routes have been developed to explore the preparation of mesoporous titania nanostructures with hierarchical morphologies and high specific surface areas. One of the most promising and simple methods for synthesizing such titania nanostructures is the template method. Using core template method and sol-gel process, core-shell structures are obtained. The subsequent removal of the templates by either heat treatment or solvent extraction, then, yields template-directed and

Table 1 Anatase content, crystallite size, specific surface area, pore volume and mean particle size of synthesized titania nanoparticles prepared by sol-gel method.

Samples	TIP (ml)	Ethanol (ml)	HCl (ml)	H ₂ O (ml)	Specific surface area (m ² /g)	Pore volume (cc/g)	Mean pore size (nm)	% Anatase	crystallite size (nm)	
									Anatase	Rutile
E1 ¹⁴	5.5	54.8	1.68	19	29	0.08	11	20	15	20
E2	5.5	54.8	1.68	3.3	33	0.11	14	70	24	31
E3	5.5	21.1	1.68	3.3	28	0.14	19	31	21	20
E1-CaCO ₃	5.5	54.8	1.68	19	265	1.58	24	14	6	10
E1-CTAB	5.5	54.8	1.68	19	80	0.37	19	92	9	31

meso-porous nanostructures. Various templates such as CaCO₃¹⁵, styrene-acrylic acid copolymer¹⁶, and cetyltrimethylammonium bromide (CTAB)¹⁷ have been successfully used.

Since the photocatalytic reaction is dictated by the properties of titania nanoparticles, it is significant to understand the factors affecting the sol-gel reactions. Our previous work¹⁴ has reported that the hydrolysis rate and calcination temperature had crucial effects on crystalline phases and pore characteristics of synthesized titania. High crystalline anatase phase with high photocatalytic activity was achieved at calcination temperature of 500 °C. In this study, we reported the influence of precursor ratios on the properties of sol-gel derived titania nanoparticles. The preparation of mesoporous titania with CaCO₃ nanoparticles or CTAB cationic surfactant as templates was also studied.

METHODS

Synthesis

In this study, titania nanoparticles were prepared by sol-gel method, employing tetraisopropoxide (Ti[OCH(CH₃)₂]₄; TIP) as a starting precursor. Ethanol and water were employed as solvents, and HCl as an acidic catalyst. The volume ratios of precursors are listed in Table 1. E1 represents samples synthesized with large excess water in sol preparation¹⁴. In E3, the water content is equal to E2, but less amount of ethanol solvent is added.

Using a sol-gel method, TIP was first dissolved in ethanol. The mixture of distilled water and HCl was then added dropwise under vigorous stirring at room temperature. The mixture was further stirred for 3 h, and the obtained gels were centrifuged, washed to remove excess reactants and catalyst, and dried at 80 °C for 24 h. Following the drying process in the oven, the samples were calcined at 500 °C for 3 h at a heating rate of 5 °C/min.

For template-assisted sol-gel preparation, commercial CaCO₃ nanoparticles by precipitation method

(NPCC101, average particle size of 40 nm) and cetyltrimethylammonium bromide (CTAB) were used as inorganic and organic templates, respectively. The main preparation of templated titania was similar to the procedure described above. The additional step is to add 14.41 g CaCO₃ into the TIP-ethanol mixture or to dissolve 1.66 g CTAB in water at 40 °C before mixing with HCl. The CaCO₃ and CTAB were completely removed by dissolving TiO₂/CaCO₃ nanostructures in diluted HCl solution overnight after calcination, while the CTAB was subsequently burned out during calcination process.

Characterization

The morphology and size of the particles were observed by transmission electron microscopy (TEM, JEOL JEM-1230). Approximately 50 randomly selected particles from each samples were imaged from different areas. Assuming particles are spherical, diameters of each particle were measured, and particle size distribution could be estimated. X-ray diffraction (XRD) patterns were recorded on a BRUKER AXS: D8DISCOVER system using Cu K α radiation to analyse the crystal structure. The average crystallite sizes of anatase and rutile were estimated by employing Debye-Scherrer equation. The fraction of anatase phase is¹⁸ $(1 + I_R/0.8I_A)^{-1}$, where I_A and I_R are the intensity of strongest diffraction line of anatase (101) and rutile (110) phase, respectively. N₂ adsorption and desorption experiments were conducted using Autosorb-1 instrument (Quantachrome, USA). The pore characteristics and specific surface area were determined using Brunauer-Emmett-Teller and Barrett-Joyner-Halenda methods, respectively.

Photocatalytic Test

The photocatalytic activity of synthesized TiO₂ nanoparticles was evaluated by measuring the photocatalytic degradation of methylene blue under UVC light irradiation (20 W UVC UV Tokiva lamp, λ_{\max} = 254 nm). Methylene blue is generally used for this

purpose due to its stability under typical environmental conditions and against UV irradiation^{19,20}. In addition, due to its molecular size, it is likely to be adsorbed in porous materials with meso-pores or macro-pores. All batch equilibrium experiments were conducted in the dark. In a typical experiment, 0.031 g of TiO₂ nanoparticles was added to 50 ml of 2×10^{-5} M methylene blue aqueous solutions. The suspensions were centrifuged, and the concentration of methylene blue was determined from the absorbance at $\lambda = 664.5$ nm, using a UV-Vis spectrophotometer (Shimadzu UV-1800). The percentage of methylene blue degradation (MB degradation) was calculated as $(1 - C/C_0)$, where C_0 is the initial concentration and C is the concentration of methylene blue solution.

RESULTS AND DISCUSSION

XRD patterns of calcined titania nanoparticles and the corresponding data of XRD crystallite size are shown in Fig. 1 and Table 1, respectively. The results show that, for template-free synthesis (E1–E3 samples), E2 titania consists of the highest content of anatase and the largest anatase and rutile crystallites. Based on previous work^{18,21}, the rate of hydrolysis reaction increases with increasing water content, and as a result, the fast hydrolysis reaction in E1 samples would produce fine particles. However, these particles are likely to agglomerate into larger particles. The estimation of particle size distribution by TEM analysis (Fig. 2) consistently shows a wide distribution ranging from 8 nm up to 100 nm. The disagreement in the particle size by TEM and crystallite size by XRD (15–20 nm) of E1 samples indicates a significant agglomeration of the synthesized titania nanoparticles. In addition to the effects on particle size and agglomeration, the amount of anatase formation generally decreases with an increase in hydrolysis rate²². From XRD results, the phase transformation of anatase to rutile is more favourable with increasing water content (E1 > E2). A small amount of ethanol in E3 samples, however, is likely to suppress the hydrolysis reaction, resulting in smaller particles and less anatase phase, compared to E2 samples.

For CTAB-templated titania, it is evident that most of the nanoparticles are more loosely-packed with increased pore volume (Fig. 2 and Table 1). The XRD pattern (Fig. 1) reveals that the synthesized titania is composed of anatase as the predominant phase with the presence of small amounts of rutile and brookite crystallites. The fraction of anatase phase is about 92%, according to the equation above. The result illustrates that CTAB template not only induces

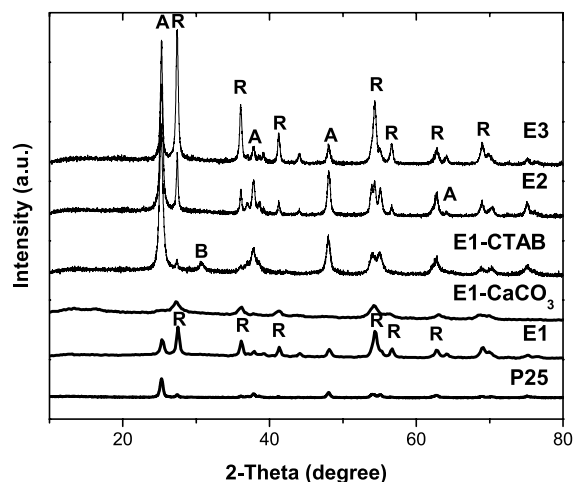


Fig. 1 XRD patterns of E1¹⁴, E2, E3, E1-CTAB, and E1-CaCO₃ titania nanoparticles, compared to commercial P25 titania.

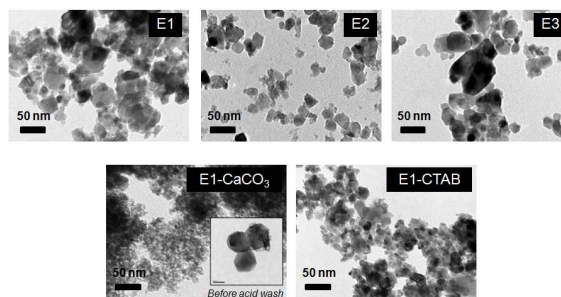


Fig. 2 TEM images of E1¹⁴, E2, E3, E1-CTAB, and E1-CaCO₃ titania nanoparticles (scale bar: 50 nm).

the formation of small and uniform anatase crystallites but also generates crystalline brookite. In general, the anatase-to-rutile phase transformation depends on several factors including the size of anatase crystallites, the existence of brookite phase, and the packing of titania nanocrystals^{23–26}. It is expected that the loose packing here has a predominant influence, and therefore inhibits the transformation from anatase to rutile phases. An increase in anatase content upon the addition of CTAB surfactant is in agreement with previous work^{27,28}.

With CaCO₃ as a template (E1-CaCO₃), on the other hand, the related XRD pattern shows very broad peaks of rutile as well as weak peaks of anatase (14%) (Fig. 1). In contrast to CTAB template, the existence of CaCO₃ nanoparticles during the calcination could act as a lot of nucleating sites for the rutile formation due to the existence of defects and vacancies. As a

result, rutile transformation was kinetically promoted, and high percentage of rutile phase was obtained. This observation is similar to the studies on the anatase-rutile phase transformation in the presence of various oxides as nucleating agents^{29,30}. In general, CaCO₃ nanoparticles, as a structure-directing agent, play an important role in the formation of the hollow or porous structure. The TEM image of E1-CaCO₃ sample is shown in Fig. 2. The inset of the TEM image shows TiO₂/CaCO₃ nanoparticles before HCl acid wash. The spherical core-shell nanostructures have diameters in the range of 85–100 nm. After the removal of CaCO₃ template, the image reveals that titania nanoparticles are actually assembled from nanocrystal subunits. This observation is consistent with the value of crystallite size (~10 nm), calculated from (110) rutile reflection peak using Scherrer equation.

Fig. 3 and Fig. 4 show the nitrogen adsorption-desorption isotherms and the pore size distributions, respectively. The template-free titania nanoparticles calcined at 500 °C exhibits a type IV adsorption isotherm, which is a characteristic of mesoporous materials. A slight increase in adsorption between $P/P_0 = 0.95$ and 1.00 indicates that all of the calcined nanoparticles exhibit a small amount of macroporosity, which can be attributed to N₂ adsorption between nanoparticles. While E1 and E2 samples show monomodal pore size distribution, the pore size distribution of E3 samples tends to be bimodal with larger mean pore size. Although less water content, the ethanol content in E3 samples was very low. A decrease in ethanol then accelerates the gelation process, causing uncontrolled pore size distribution. The specific surface areas of E1, E2, and E3 samples are in the range of 28–33 m²/g.

For CTAB-templated samples (E1-CTAB), specific surface area and an average pore diameter are approximately 80 m²/g and 19 nm, respectively (Table 1). The adsorption and desorption isotherm shows a hysteresis loop over a wide range of relative pressure due to the presence of some micro- and macro-pores (Fig. 4). Based on previous work, CTAB may play a crucial role in preventing the condensation reaction and to effectively control the morphology of sol-gel derived nanoparticles^{31,32}. The isotherm of E1-CaCO₃, on the other hand, shows a typical type-III pattern, which describes an adsorption on macropores materials. The highest specific surface area of 265 m²/g was obtained in this sample with an average pore diameter of 24 nm.

The photocatalytic property of titania nanoparticles was examined by measuring the photodegradation of methylene blue in an aqueous suspension

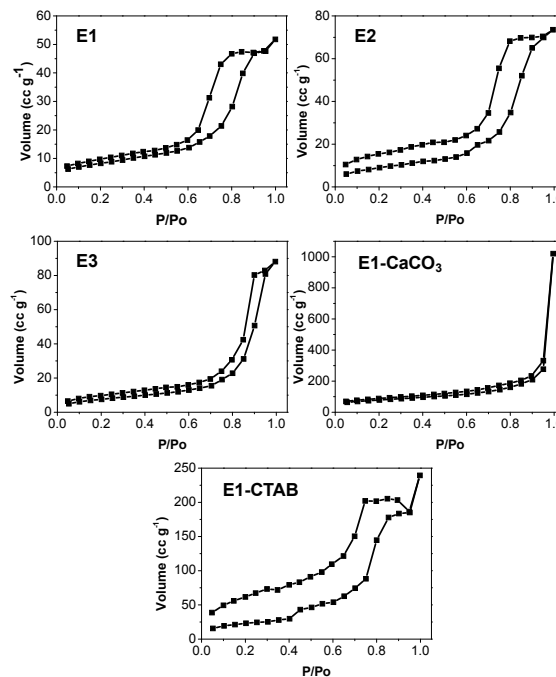


Fig. 3 N₂ adsorption-desorption isotherms of E1¹⁴, E2, E3, E1-CTAB, and E1-CaCO₃ titania nanoparticles.

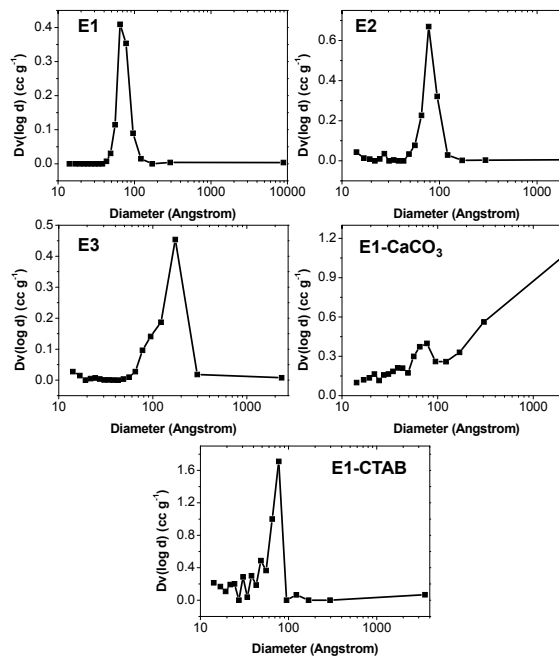


Fig. 4 Pore size distribution of E1¹⁴, E2, E3, E1-CTAB, and E1-CaCO₃ titania nanoparticles.

of titania. High anatase crystallinity typically helps to promote the separation between the photo-excited

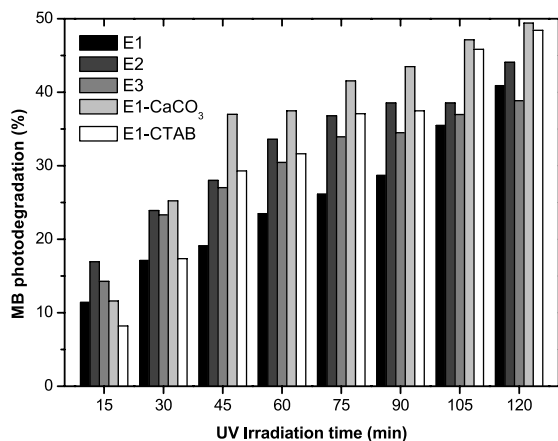


Fig. 5 The percentages of methylene blue photodegradation in different aqueous titania suspensions at different irradiation times.

electrons and holes, while high specific surface area in conjunction with suitable pore size would enhance the adsorption of organic molecules on the surface of photocatalysts³³. The results show that the amount of methylene blue photodegradation increases in the sequence of E1-CaCO₃ > E1-CTAB > E2 > E1 > E3. Based on the analysis of XRD patterns and pore characteristics, it can be concluded that the photocatalytic activity of titania depends on pore characteristics and the amount of anatase crystallite. Large number of micropores with sizes are comparable to the molecular size of methylene blue in E1-CTAB, however, can limit their adsorption and hence photocatalysis processes. Pure rutile titania nanoparticles do not typically exhibit photocatalytic activity of organic solution³⁴.

CONCLUSIONS

The effects of precursor composition and templates on the crystal structure, crystallinity, crystallite size, and photocatalytic activity were investigated. The specific surface area of template-free titania nanoparticles prepared from different precursor compositions and calcined at 500 °C were not much different. However, samples with high amount of anatase crystallite were likely to have higher photocatalytic activities. High specific surface area of more than 250 m²/g titania was achieved with CaCO₃ template-assisted sol-gel method. However, the presence of CaCO₃ nanoparticles during calcination can act as a nucleating agent for the formation of rutile with low crystallinity and small crystallite size. High photocatalytic activities observed in CaCO₃- and CTAB-templated titania were

predominantly due to appropriate pore characteristics (i.e., high specific surface) and high content of anatase crystallites, respectively.

Acknowledgements: This work is financially supported by Silpakorn University Research and Development Institute. The authors wish to thank Department of Materials Science and Engineering, Faculty of Engineering and Industrial Technology, Silpakorn University, and National Centre of Excellence for Petroleum, Petrochemicals and Advanced Materials for supporting and encouraging this investigation. We also would like to express our special and sincere gratitude to Dr Pat Sooksaen, Department of Materials Science and Engineering, Faculty of Engineering and Industrial Technology, Silpakorn University, for his valuable and constructive comments and for his important support throughout this study.

REFERENCES

- Grätzel M (2003) Review: Dye-Sensitized Solar Cells. *J Photochem Photobiol C Photochem Rev* **4**, 145–53.
- Thompson TL, Yates J Jr (2006) Surface science studies of the photoactivation of TiO₂-New photochemical processes. *Chem Rev* **106**, 4428–53.
- Pal M, Garcya Serrano J, Santiago P, Pal U (2007) Size-controlled synthesis of spherical TiO₂ nanoparticles: Morphology, crystallization, and phase transition. *J Phys Chem C* **111**, 96–102.
- Wang G (2007) Hydrothermal synthesis and photocatalytic activity of nanocrystalline TiO₂ powders in ethanol-water mixed solutions. *J Mol Catal A* **274**, 185–91.
- Sahni S, Reddy B, Murty B (2007) Influence parameters on the synthesis of nano-titania by sol-gel route. *Mater Sci Eng A* **452-453**, 758–62.
- Rao AR, Dutta V (2007) Low-temperature synthesis of TiO₂ nanoparticles and preparation of TiO₂ thin films by spray deposition. *Sol Energ Mater Sol Cell* **91**, 1075–80.
- Park JY, Lee C, Jung KW, Jung D (2009) Structure related photocatalytic properties of TiO₂. *Bull Kor Chem Soc* **30**, 402–4.
- Liu J, Qin W, Zuo S, Yu Y, Hao Z (2009) Solvothermal-induced phase transition and visible photocatalytic activity of nitrogen-doped titania. *J Hazard Mater* **163**, 273–8.
- Mastali Khan Tehrani F, Rashidzadeh M, Nemati A, Irandoukht A (2011) Factors influencing the preparation of TiO₂ nanopowders from titania. *Ceram Silikaty* **55**, 31–5.
- Yang J, Mei S, Ferreira JMF (2001) Hydrothermal and synthesis of TiO₂ nanopowders from tetraalkylammonium hydroxide peptided sols. *Mater Sci Eng C* **15**, 183–5.
- Tong T, Zhang J, Tian B, Chen F, He D (2008) Preparation and characterization of anatase TiO₂ microspheres

- with porous frameworks via controlled hydrolysis of titanium alkoxide followed by hydrothermal treatment. *Mater Lett* **62**, 2970–2.
12. Sayilkan F, Asiltürk M, Sayilkan H, Önal Y, Akarsu M, Arpaç E (2005) Characterization of TiO₂ synthesized in alcohol by a sol-gel process: the effects of annealing temperature and acid catalyst. *Turk J Chem* **29**, 697–706.
 13. Spurr RA, Myers H (1957) Quantitative analysis of anatase-rutile mixture with a X-ray diffractometer. *Anal Chem* **29**, 760–2.
 14. Loryuenyong V, Angamnuaysiri K, Sukcharoenpong J, Suwannasri A (2012) Sol-gel derived mesoporous titania nanoparticles: Effects of calcination temperature and alcoholic solvent on the photocatalytic behavior. *Ceram Int* **38**, 2233–7.
 15. Bala H, Yu Y, Zhang Y (2008) Synthesis and photocatalytic oxidation properties of titania hollow spheres. *Mater Lett* **62**, 2070–3.
 16. Wang D, Song C, Liu Y, Hu Z (2006) Preparation and characterization of TiO₂ hollow spheres. *Mater Lett* **60**, 77–80.
 17. Lee DU, Jang SR, Vittal R, Lee J, Kim KJ (2008) CTAB facilitated spherical rutile TiO₂ particles and their advantages in a dye-sensitized solar cell. *Sol Energ* **82**, 1042–8.
 18. Bernards TNM, van Bommel MJ, Boonstra AH (1991) Hydrolysis-condensation processes of the tetraalkoxysilanes TPOS, TEOS and TMOS in some alcoholic solvents. *J Non Cryst Solids* **134**, 1–13.
 19. Yogi Ch Kojima K, Wada N, Tokumoto H, Takai T, Mizoguchi T, Tamiaki H (2008) Photocatalytic degradation of methylene blue by TiO₂ film and Au particles-TiO₂ composite film. *Thin Solid Films* **516**, 5881–4.
 20. Jian-xiao LV, Ying Cui Guo-hong Xie Ling-yun Zhou Su-fen Wang (2011) Decoloration of methylene blue simulated wastewater using a UV-H₂O₂ combined system. *J Water Reuse Desalination* **1**, 45–51.
 21. Mine E, Nagao D, Kobayashi Y, Konno M (2005) Solvent effects on particle formation in hydrolysis of tetraethyl orthosilicate. *J Sol Gel Sci Tech* **35**, 197–201.
 22. Sing KSW, Everett DH, Haul RAW, Moscow L, Pierotti RA, Rouquerol J, Siemieniewska T (1985) Reporting physisorption data for gas/solid systems with special reference to the determination of surface area and porosity. *Pure Appl Chem* **57**, 603–19.
 23. Zheng R, Meng X, Tang F (2009) Synthesis, characterization and photodegradation study of mixed-phase titania hollow submicrospheres with rough surface. *Appl Surf Sci* **255**, 5989–94.
 24. Wang P, Chen D, Tang FQ (2006) Preparation of titania-coated polystyrene particles in mixed solvents by ammonia catalysis. *Langmuir* **22**, 4832–5.
 25. Zhang H, Banfield JF (1998) Thermodynamic analysis of phase stability of nanocrystalline titania. *J Mater Chem* **9**, 2073–6.
 26. Hu Y, Tsai HL, Huang LC (2003) Effect of brookite phase on the anatase-rutile transition in titania nanoparticles. *J Eur Ceram Soc* **23**, 691–6.
 27. Liu GQ, Jin ZG, Liu XX, Wang T, Liu ZF (2007) Anatase TiO₂ porous thin films prepared by sol-gel method using CTAB surfactant. *J Sol Gel Sci Tech* **41**, 49–55.
 28. Benkacem T, Agoudjil N (2008) Synthesis of mesoporous titania with surfactant and its characterization. *Am J Appl Sci* **5**, 1437–41.
 29. Gennari FC, Pasquevich DM (1998) Kinetics of the anatase-rutile transformation in TiO₂ in the presence of Fe₂O₃. *J Mater Sci* **33**, 1571–8.
 30. Shannon RD, Pask JA (1965) Kinetics of the anatase-rutile transformation. *J Am Ceram Soc* **48**, 391–8.
 31. Luo S, Wang F, Shi Z, Xin F (2009) Preparation of highly active photocatalyst anatase TiO₂ by mixed template method. *J Sol Gel Sci Tech* **52**, 1–7.
 32. Benkacem T, Agoudjil N (2008) Synthesis of mesoporous titania with surfactant and its characterization. *Am J Appl Sci* **5**, 1437–41.
 33. Ohtani B, Ogawa Y, Nishimoto SI (1997) Photocatalytic activity of amorphous-anatase mixture of titanium(IV) oxide particles suspended in aqueous solutions. *J Phys Chem B* **101**, 3746–52.
 34. Zheng R, Meng X, Tang F (2009) Synthesis, characterization and photodegradation study of mixed-phase titania hollow submicrospheres with rough surface. *Appl Surf Sci* **255**, 5989–94.